FM 8773 (1994)

To be held in the files of JFM

APPENDICES TO

On one-dimensional flow of a conducting gas between electrodes - with application to MHD thrusters

By M.D. Cowley and J.H. Horlock

August 1993

Appendix A. The (B,ρ)-curves

In this appendix we seek to establish how the magnetic field B varies with the density ρ of a perfect gas in the MHD duct. Although some results were proved in §3 (such as B being stationary at a sonic point), the fact that there are three main types of (B,ρ)-curve, (a), (b) and (c) in figure 4, was not fully justified.

For ease of reference we repeat equations (7), (9) and (8) for continuity, momentum and energy respectively:

$$\rho u = G , \tag{A1}$$

$$p + \rho u^2 = F = F^o - B^2/2\mu , \tag{A2}$$

$$h + u^2/2 = H = H^o - EB/\mu G , \tag{A3}$$

where G, F^o, H^o and E are constant along a duct of constant cross-sectional area. Elimination of B between equations (A2) and (A3) yields

$$F^o - F = (G^2\mu/2E^2)(H^o - H)^2 , \tag{A4}$$

which describes a parabola on the (H,F)-plane (see figure A2), having its vertex at (H^o,F^o) and axis on $H = H^o$. We shall refer to this as the process parabola.

To determine how variables other than H and F vary along the process parabola we make use of the properties of the (H,F)-plane illustrated on figure A1, which have been derived for other magnetogasdynamic investigations (Cowley 1963 and 1967).

To recapitulate, the starting point is the fact that a normal shock wave links two states with identical values of G, F and H. There is a limit to the range of F for this at given G and H since G and H constant define a Fanno process and F is maximum at sonic conditions (Shercliff 1958)- a fact already quoted in §3. Similarly the range of H is limited because a Rayleigh process with G and F constant has F minimum at sonic conditions (Shercliff 1958). It follows that there is a sonic-state line on the (H,F)-plane, below which no real flow state exists. The equation of the line is found from the definitions of G, F and H in (A1), (A2) and (A3), together with the perfect-gas results $p = \rho a^2/\gamma$ and $h = a^2/(\gamma - 1)$ and with the sonic condition $u = a$:

$$\text{sonic-state line} \qquad F^2 = 2\{(\gamma^2 - 1)/\gamma^2\}G^2H \ . \tag{A5}$$

Above the sonic-state line, each point (H,F) for given G defines a supersonic and a subsonic state, being the upstream and downstream states of a normal shock wave, but there is another limit associated with the fact that not all subsonic states can be reached by a shock wave. There will be a line corresponding to infinite Mach number at the supersonic state, which is found by setting $p = 0$ and $h = 0$ in the definitions of F and H to give

$$\text{hypersonic-state line} \qquad F^2 = 2G^2H \ . \tag{A6}$$

Above this line each point (H,F) for given G defines only a subsonic state, but this region extends to the F-axis, where conditions are h and u zero, ρ infinite and p finite, and it also extends to $F \to \infty$, where conditions are u zero, ρ and p infinite, but h finite.

The sonic-state (A5) and hypersonic-state (A6) lines are

summarized on figure A1.

Consider values of H^o and F^o such that part of the process parabola (A4) lies above the sonic-state parabola (A5), as sketched on figure A2. The two parabolas must intersect at either one or two or three points where H and F are positive (see figure A4 later). Take first the case sketched in figure A2 with two intersection points S_1 and S_2. Points on the process parabola to the left of its vertex represent states with B positive ($H < H^o$ with E assumed positive in equation (A3)), while states to the right have B negative. There are two tangents common to the process and sonic-state parabolas, with contact points R_1, R_2 on the process curve and T_1, T_2 on the sonic-state line, as shown on figure A2. The implication is that density is stationary at R_1 and R_2 and, since the slope of the constant density lines increases with ρ, R_1 and R_2 give states with ρ maximum and ρ minimum respectively. Consideration of the slopes of the other tangents to the sonic-state parabola passing through R_1 and R_2 shows that the maximum ρ state is subsonic and the minimum ρ state is supersonic.

The process parabola of figure A2 corresponds to B reducing through a succession of subsonic states from sonic at S_1, while ρ increases up to R_1, but thereafter decreases. The succession of subsonic states continues with B passing through zero at the vertex of the process parabola and finally reaching a minimum at sonic state S_2. Similarly there is a continuous succession of supersonic states from S_1 to S_2 with ρ passing through a minimum at R_2, provided that the process parabola lies below the hypersonic-state line. When the process is mapped onto the (B,ρ)-plane, it will clearly give what was designated in §3 as

the closed loop of a type (a) curve (see figure 4). Note that the sonic point S_2 is not necessarily to the right of the process-parabola vertex. S_2 could be at the vertex (i.e. B = 0 at that sonic state) or even to the left of the vertex (i.e. B positive).

From equation (18) of §3 it was easy to see that values of B for given ρ are symmetrically disposed about $\{(\gamma - 1)/\gamma\}(E/G)\rho$. There is a geometrical argument for proving this result direcly from the (H,F)-plane analysis, as illustrated by figure A3. Consider a constant-ρ line which intersects the process parabola at P_1 and P_2. By evaluating the slope of the line from the co-ordinates of P_1 and P_2, we obtain

$$\left(\frac{EB_2}{\mu G} - \frac{EB_1}{\mu G}\right)\left(\frac{\partial F}{\partial H}\right)_\rho = \frac{B_2^2}{2\mu} - \frac{B_1^2}{2\mu} ,$$

i.e.

$$\left(\frac{\gamma - 1}{\gamma}\right)\frac{E\rho}{G} = \frac{1}{2}(B_1 + B_2) , \qquad (A9)$$

where we have made use of equation (A7) for the slope of the constant-density line.

An outstanding question is whether there are conditions such that a portion of the process parabola between the sonic points S_1 and S_2 on figure A2 can lie above the hypersonic-state line, so that the corresponding (B,ρ)-curve would not be a closed loop, some supersonic states having been lost. We shall defer the answer until the next appendix.

We now turn to cases where the process and sonic-state parabolas intersect once or thrice where H and F are both positive. The possibilities are illustrated by the family of curves sketched

in figure A4. The process parabola (a) on that figure has sonic states marked S_1 and S_2 and flow behaviour between them will be the same as discussed above in connection with the sketch of figure A2. However, now the extension of the process parabola to the left is shown with a third sonic-state point S_3 and there will necessarily be an intersection with the hypersonic-state parabola further to the left. The extension beyond S_3 represents a continuous succession of subsonic flow states from zero velocity on the F-axis to sonic, with B and ρ decreasing, and a continuous succession of supersonic flow states from hypersonic to sonic, with B decreasing (there may or may not be a point of minimum ρ). However, since the extension is not connected via real states (i.e. on the dashed line in figure A4) to the part of the process parabola which lies between S_1 and S_2, it will form a separate branch when mapped onto the (B,ρ)-plane. Note that B and ρ are greater on the extension than any values on the part between S_1 and S_2 so that the extension forms an upper branch and that the slopes of the parabolas at S_3 show that B is less than $\{(\gamma - 1)/\gamma\}(E/G)\rho$ there. The (B,ρ)-curve is sketched on figure A5 with its lower closed loop and upper branch. The disposition of the curve has been chosen to illustrate a feature mentioned above as a possibility in connection with the curve of figure A2, namely a curve having $B = 0$ at a sonic state because the vertex of the process parabola in the (H,F)-plane coincides with S_3.

If the vertex of the process parabola is raised sufficiently, a curve such as that labelled (c) on figure A4 is obtained with only one sonic-state point. For the disposition shown $(F^o - F) = B^2/2\mu$ reaches a maximum there, but, since B is negative (to

the right of the axis of the process parabola), B is a minimum. The process and sonic-state parabolas do have a common tangent, with contact point on the former corresponding to a supersonic state (see the properties of the (H,F)-plane on figure A1), so that ρ is a minimum at that point. The succession of supersonic and subsonic states on the process parabola end at the left hypersonically and with $u = 0$ respectively. It is clear that when the process is mapped onto the (B,ρ)-plane, the shape of the (c) curve will in most respects be similar to the upper branch of the (a) curve and this is illustrated in figure A5. There is a possibility that the process parabola intersects the hypersonic-state line thrice in a similar manner to the way in which the (a) curve on figure A4 intersects the sonic-state line, but, in the context of our assumed conditions of subsonic or sonic inlet and supersonic or sonic exit (see §4 and Appendix B) only subsonic flow on a type (c) curve is of interest and the possibility is of no concern.

A process parabola labelled (b) is sketched on figure A4, which just touches the sonic-state parabola. It is clearly transitional, the sonic points S_1 and S_3 of type (a) curves having merged before disappearing as type (c) curves are formed. The corresponding (B,ρ)-curve of figure A5 therefore exhibits a sonic branch point or crossover. By equating expressions for the slopes of the process and sonic-state parabolas, we obtain the result of §3 that $E/uB = \rho E/GB = \gamma/(\gamma - 1)$ at the crossover.

The above discussion has not been exhaustive. We have not, for example, given a sub-categorization, based on whether there are or are not states having $B < 0$. We hope that a sufficient outline has been given so as to make obvious any other features

of possible (B,ρ)-variation.

Appendix B. Parameterization of the (B,ρ)-curves

In §4 we presented a map of the different flow regimes which would occur in the MHD duct for different values of a magnetic field parameter β^* and an electric field parameter λ^* (see equation (21a) for definitions and figure 5 for the map). This appendix is intended to provide a firmer basis for the map than the previous discussion. However, in the first instance, it is easier to develop the argument in terms of parameters which relate directly to local duct conditions (rather than to the plenum-chamber state, as β^* and λ^* do) and which also relate directly to the analysis of the (H,F)-plane.

For a perfect gas any non-dimensional flow variable, such as Mach number may be taken as depending on the non-dimensional grouping of G, F and H, i.e G^2H/F^2 (subject to the ambiguity of whether the state is supersonic or subsonic), and γ. From equations (A1), (A2) and (A3), together with the perfect-gas relations, we obtain

$$\frac{G^2H}{F^2} = \frac{\gamma^2}{2(\gamma - 1)} \frac{M^2\{2 + (\gamma - 1)M^2\}}{(\gamma M^2 + 1)^2} . \qquad (B1)$$

Thus, for example, the value of G^2H/F^2 at a sonic state is $\gamma^2/2(\gamma^2 - 1)$, as in equation (A5).

We choose to characterize the magnetic field by $B^2/2\mu F^o$. Using equation (A2) and the perfect-gas relations, F^o may be expressed in terms of properties at inlet to the duct ρ_o, u_o, M_o, if we require to do so:

$$\frac{B^2}{2\mu F^o} = \frac{B^2/\mu\rho_o u_o^2}{B^2/\mu\rho_o u_o^2 + 2(1 + \gamma M_o^2)/\gamma M_o^2} . \qquad (B2)$$

From equations (A1), (A2) and (A3) the new parameters describing the flow and field state are related by

$$\frac{GE}{\sqrt{(\mu F^{o3}/2)}} - \left(\frac{G^2H^o}{F^{o2}}\right)\left(\frac{\sqrt{(2\mu F^o)}}{B}\right) = -\left(\frac{G^2H}{F^2}\right)\left(1 - \frac{B^2}{2\mu F^o}\right)^2\left(\frac{\sqrt{(2\mu F^o)}}{B}\right) , \qquad (B3)$$

which introduces two parameters to characterize the particular process, G^2H^o/F^{o2} and $GE/\sqrt{(\mu F^{o3}/2)}$. The first of these controls where the vertex of the process parabola lies in the (H,F)-plane. The second is clearly an electric-field parameter with the useful property of increasing if the electric field is increased for otherwise fixed inlet conditions.

Equation (B3) gives a straight line in the $(G^2H^o/F^{o2}, GE/\sqrt{(\mu F^{o3}/2)})$-plane for given local values of G^2H/F^2 (flow state) and $B^2/2\mu F^o$ (magnetic-field state), and the line forms the locus of all process-parameter values which permit that particular flow and magnetic-field condition to exist in the process. Note that the slope of the locus is equal to $\sqrt{(2\mu F^o/B^2)}$.

The straight lines of equation (B3) for given G^2H/F^2 have an envelope, for which we obtain the following equations, parametric in $B^2/2\mu F^o$:

$$\frac{G^2H^o}{F^{o2}} = \left(\frac{G^2H}{F^2}\right)\left(1 - \frac{B^2}{2\mu F^o}\right)\left(1 + 3\frac{B^2}{2\mu F^o}\right) , \qquad (B4a)$$

$$\frac{GE}{\sqrt{(\mu F^{o3}/2)}} = 4\left(\frac{G^2H}{F^2}\right)\left(\frac{B}{\sqrt{(2\mu F^o)}}\right)\left(1 - \frac{B^2}{2\mu F^o}\right) . \qquad (B4b)$$

The envelope is found to be a curvilinear triangle, as shown in figure B1, with sides concave looking from the outside. Although only parameter points with positive $GE/\sqrt{(\mu F^{o3}/2)}$ are of interest, the envelope of loci for state points with $B < 0$ (i.e. negative-slope locus) is below the G^2H^o/F^{o2} axis and is therefore included in the figure. Various properties of the envelope curve are easily found and we list some of the important ones mainly for future reference:

(i) The cusps at the ends of the right-hand curvilinear side of the envelope are at $G^2H^o/F^{o2} = (4/3)(G^2H/F^2)$, $GE/\sqrt{(\mu F^{o3}/2)} = \pm(8/\sqrt{27})(G^2H/F^2)$. The slope of a tangent at the upper cusp is $\sqrt{3}$.

(ii) The envelope cuts the horizontal axis at $G^2H^o/F^{o2} = G^2H/F^2$ and the tangent there corresponds to a locus of parameter values for there to be a $B = 0$ state at the given G^2H/F^2. (Note the implication of an alternative interpretation of G^2H^o/F^{o2}, as the exit value of G^2H/F^2.

(iii) The $B = 0$ state line intersects with the upper side of the envelope at $GE/\sqrt{(\mu F^{o3}/2)} = \sqrt{(32/27)}(G^2H/F^2)$. The slope of the tangent there is $\sqrt{(3/2)}$.

(iv) The slopes of the upper and lower sides of the envelope are ± 1 at the origin.

The method of determining which type of (B,ρ)-curve is to be associated with a particular parameter point is to count how many tangents can be drawn to the envelope of *sonic-state loci*. That number gives the number of sonic points: two for a type (a) curve without an upper branch, three for type (a) with upper

branch and one for type (c). Using this method the figure has been marked to show which regions of the parameter space give process curves with zero, one, two or three sonic points.

Conditions for a transitional type (b) curve merit further discussion. There is no ambiguity over the fact that such a curve has two sonic points, because the one which is a branch point or crossover occurs as the limit when two sonic points of a type (a) curve with upper branch merge. The corresponding behaviour in the $(G^2H^o/F^{o2}, GE/\sqrt{(\mu F^{o3}/2)})$-plane is for a parameter point to approach the upper side of the curvilinear triangle from the region for three sonic states. As it does so, the two tangents to the upper side merge into one. The (B,ρ)-curve of type (b) is therefore to be associated with parameter points *on* the upper side of the curvilinear triangle itself.

The question then arises as to the meaning of parameter points lying on the right-hand side of the curvilinear triangle. As the side is approached from the two-sonic-state region, the corresponding (B,ρ)-behaviour is for a type (a) closed loop to shrink to a point. (There is a small length where the side may be approached from a three-sonic-state region, but consideration of the ordering of B between the tangents shows that behaviour still corresponds to shrinking of a closed loop.) When a parameter point lies on the envelope for sonic-state loci, it is easily shown that equation (B4b) is equivalent to the result quoted in §3 for a sonic-state crossover, namely $E/uB = \gamma/(\gamma - 1)$.

We shall refer mainly to the envelope for sonic-state loci, but the same procedure as above may be used to determine whether a

state with a particular Mach number other than unity appears on a process curve, G^2H/F^2 in equations (B4) being given the appropriate value for the Mach number (equation (B1)). Note that one envelope can serve for two Mach numbers, one greater than unity and the other less, for upstream and downstream states of a normal shock wave respectively. Important special cases are the envelope for hypersonic-state loci with $G^2H/F^2 = 1/2$ and the envelope curve for $M = 0$. In the latter case the envelope shrinks to a point at the origin of the parameter space and any line through the origin with positive slope greater than unity is a tangent to it, so that either one or zero $M = 0$ states are possible, depending on whether the parameter point lies above or below the tangent with slope unity.

There is one other important condition to establish in the parameter space, namely that for there to be a magnetosonic state in the process. For a point where $u^2 = a^2 + B^2/\mu\rho$ and $E/uB = \rho E/GB = 1$ (see equation (16) of §3), equations (A2) and (A3) give

$$F^o = (\rho u^2 - B^2/\mu)/\gamma + \rho u^2 + B^2/2\mu \ , \qquad \text{(B5a)}$$

$$H^o = \frac{u^2 - B^2/\mu\rho}{\gamma - 1} + u^2/2 + B^2/\mu\rho \ . \qquad \text{(B5b)}$$

From equations (A1), (B5a) and (B5b), together with $E = uB$, we can form

$$\frac{G^2H^o}{F^{o2}} = \left[\frac{\gamma^2}{2(\gamma^2 - 1)}\right] 2 \left(\frac{1 - 2(2 - \gamma)\beta/(\gamma + 1)}{\{1 - (2 - \gamma)\beta/(\gamma + 1)\}^2}\right) , \qquad \text{(B6a)}$$

$$\frac{GE}{\sqrt{(\mu F^{o3}/2)}} = \left[\frac{\gamma^2}{2(\gamma^2 - 1)}\right]\left(\frac{64(\gamma - 1)^2}{\gamma(\gamma+1)}\right)^{1/2} \times \left(\frac{\beta^{1/2}}{\{1 - (2 - \gamma)\beta/(\gamma - 1)\}^{3/2}}\right), \qquad \text{(B6b)}$$

where $\beta = B^2/\mu\rho u^2$. Equations (B6a) and (B6b) are parametric in β for the magnetosonic line drawn in the parameter space of figure B1. Since the axes of that figure are given in units of G^2H/F^2, the position of the line is only correct for one value of G^2H/F^2, which we have taken to be that for a sonic state, i.e. the positioning is correct when the diagram is being used to investigate how many sonic points there are on a process curve. The expressions on the right-hand sides of equations (B6a) and (B6b) will be in units of G^2H/F^2 if the expressions in square brackets are dropped. Furthermore, it may be shown that points in the parameter space lying below and to the left of the magnetosonic line would have $E < uB$ over some range of the supersonic states of a type (a) closed loop.

We now consider how parameter values must vary as the electric field is increased for given plenum-chamber state and given value of magnetic-field strength at inlet to the MHD duct (as discussed in §4, increasing the electric field corresponds to shortening the duct). Take first the parameter point O_1 of figure B2, which lies on the magneto-acoustic line in the $(G^2H^o/F^{o2}, GE/\sqrt{(\mu F^{o3}/2)})$-plane. Its position is such that two tangents can be drawn to the right-hand side of the envelope for sonic-state loci, one with negative slope and one with positive slope, i.e. the parameter values give a closed loop (B,ρ)-curve of type (a) with one sonic point where B is negative and the

other where B is positive. The point clearly corresponds to a point on AA' of the (β^*,λ^*)-plane of figure 5.

Although the sketch has the contact point of the positive-slope tangent below the cusp, i.e. tangent slope $\sqrt{(2\mu F^o/B^2)} > \sqrt{3}$ (see (i) above), a similar discussion to the following applies when the contact point lies between Q on figure B2 and the upper cusp.

All points on the positive-slope tangent through O_1 will have the same value of $\sqrt{(2\mu F^o/B^2)}$ at the sonic point associated with that locus. Therefore a sonic inlet state with constant G, F^o and $B = B_o$ can be maintained while E is raised if the parameter point is moved along that tangent, O_1P_1 of figure B2. P_1 also lies on the locus for a sonic state with B = 0, i.e.the exit condition has become sonic (see property (ii) above), corresponding to a point on the line BB' in the (β^*,λ^*)-plane of figure 5. Progress along the continuation of O_1P_1 is prohibited, because both sonic points on an associated closed-loop (B,ρ)-curve would have B positive, i.e. the loop no longer crosses the ρ axis to give a B = 0 exit state. However, as discussed in §4, the sonic inlet and exit conditions for parameter point P_1 now allow a range of flows there from fully supersonic between duct inlet and exit to fully subsonic.

After P_1 there is no possibility of further increase in E with the same plenum-chamber conditions and inlet magnetic field as before unless relaxation of the requirement of sonic state at inlet provides an opportunity. Reduction of the Mach number at inlet to the duct implies a decrease in mass flow rate and hence G. Using a well known result of one-dimensional gasdynamics

(see, for example, Shercliff 1958),

$$Tds = dH - \frac{dF}{\rho} + \frac{udG}{\rho} ,$$

where here s denotes entropy, we obtain for the variation of F^o at inlet

$$dF^o = udG . \qquad (B7)$$

In deriving equation (B7) we have used the facts that through the convergence H and s are constant at the plenum-chamber values and that $dF^o = dF$ for fixed B. It follows that moving to operation with subsonic inlet implies a *reduction* in $\sqrt{(2\mu F^o/B_o^2)}$.

Suppose that we try for a solution with a particular inlet Mach number, a point on P_1Q (sonic exit) has to be found such that there is a tangent with appropriate slope (less than the slope of O_1P_1) to an envelope curve appropriate to the Mach number (i.e. one reduced in scale by comparison with the sonic-state envelope). The parameter point will therefore lie above P_1. Although $GE/\sqrt{(\mu F^{o3}/2)}$ has thereby been increased above the value it had at P_1, it is not immediately clear that the electric field has been increased since both G and F^o are changed. However,

$$d\left(\frac{G}{\sqrt{F^{o3}}}\right) = \frac{1}{\sqrt{F^{o5}}}\left(F^o dG - \frac{3}{2}udG\right) = \frac{dG}{\sqrt{F^{o5}}}\left\{p - \frac{1}{2}\rho u^2 + \frac{B_o^2}{2\mu}\right\} , \qquad (B8)$$

using equation (B7). Since we have $p = \rho u^2/\gamma M^2$ and for subsonic flow $\gamma M^2 < 2$, the expression in braces is positive and $G/\sqrt{(\mu F^{o3}/2)}$ is reduced as G decreases. Therefore the electric field must have increased by comparison with its value at P_1.

As the parameter point progresses upwards along P_1Q, the (B,ρ)-

curve will change to one having an upper branch (see figure B1 for the three-sonic-state region) and then at Q it will change to type (c) (corresponding to being on the line CB' in the (β^*,λ^*)-plane of figure 5). However, these latter changes do not affect the nature of the flow in the duct.

There is a limit to progress of the parameter point up the continuation of P_1Q, which occurs when M = 0 at duct inlet (the KKS limit). F^o is then $p_p + B_o^2/2\mu$, where p_p is the plenum chamber pressure. The slope of the tangent to the M = 0 envelope (i.e. the origin) is $\sqrt{(1 + 2\mu p_p/B_o^2)}$ and, since P_1Q is the line $G^2H^o/F^{o2} = \gamma^2/2(\gamma^2 - 1)$, we have at the limit

$$\frac{GE}{\sqrt{(\mu F^{o3}/2)}} = \frac{\gamma^2}{2(\gamma^2 - 1)}\left(1 + \frac{2\mu p_p}{B_o^2}\right)^{1/2} . \qquad (B9)$$

With a little more algebra $GE,\sqrt{(\mu F^{o3}/2)}$ may be related to λ' and equation (33) is recovered from this result.

Consider next plenum-chamber conditions and inlet magnetic field such as to give a parameter point O_2 further up the magneto-acoustic line, as illustrated on figure B3. The tangent to the sonic-state envelope has its contact point on the upper side of the curvilinear triangle to the left of Q, which is still taken to be at the intersection of the B = 0 locus with the envelope. Property (iii) above implies that $\sqrt{(2\mu F^o/B^2)}$ is now greater than $\sqrt{(3/2)}$. Parameter points along O_2P_2 give type (a) (B,ρ)-curves and the flow regime is similar to that for points along O_1P_1. However, progress of the parameter point along the straight line which is the continuation of the tangent O_2P_2 is prohibited for the following reasons, even though the (B,ρ)-curves for points beyond P_2 still cross the ρ-axis. Consider point X on O_2P_2

extended. There are three tangents to the sonic-state envelope from X, one with negative slope and two with positive. Of the latter two tangents, XP_2 has the lesser slope, i.e. it corresponds to the higher value of B and is therefore associated with the sonic point on the upper branch of a type (a) (B,ρ)-curve. However, by continuing along O_2P_2 extended we are trying to match the inlet condition to that upper-branch sonic point and there will be no route to a possible exit state where $B = 0$ (see figure A5). Again, the only opportunity for resolution of the situation is by relaxing the condition on sonic entry to the duct.

Since any point in the vicinity of P_2 has a tangent with negative slope, the associated (B,ρ)-curve crosses the ρ-axis. The exit state must be supersonic and this can only be reached by flow from a subsonic entry if the (B,ρ)-curve is of type (b), i.e. with a crossover, the parameter point being on the sonic-state envelope. In principle such a point can be found for an inlet Mach number less than unity in the same way as was outlined for finding a parameter point in the previous case considered (on P_1Q of figure B2), but a difficulty arises. Whether the point lies to the right or the left of P_2 is not immediately obvious from the geometry and an algebraic approach is needed.

Consider a parameter point on the sonic-state envelope and suppose that the inlet state is varied so as to keep H_o (inlet H), s_o and B_o constant while G is decreased. Then

$$d\left(\frac{G^2H^o}{F^{o2}}\right) = 2\,\frac{GH_o}{F^{o2}}\,dG + \frac{B_o}{\mu F^{o2}}\,d(GE) - 2\,\frac{G^2H^ou_o}{F^{o3}}\,dG\ ,$$

where use has been made of equation (A3) to relate H^o to H_o and EB_o and of equation (B7) to relate dF^o to dG. The variation of E must be such as to keep the parameter point on the sonic-state envelope, i.e.

$$d\left(\frac{GE}{\sqrt{(\mu F^{o3}/2)}}\right) = \left(\frac{2\mu F^o}{B_c^2}\right)^{1/2} d\left(\frac{G^2H^o}{F^{o2}}\right),$$

since the slope is $\sqrt{(2\mu F^o, B_c^2)}$, where the subscript c denotes value at the crossover state. Eliminating d(GE), we obtain

$$\left(\frac{B_o}{B_c} - 1\right) d\left(\frac{G^2H^o}{F^{o2}}\right) = -2\frac{GH_o}{F^{o3}}\left(F^o - Gu_o - \frac{Eu_oB_o}{4\mu H_o}\right) dG,$$

$$= -2\frac{GH_op_o}{F^{o3}}\left\{1 + \frac{B_o^2}{2\mu p_o}\left(1 - \frac{\gamma}{\gamma - 1}\frac{u_cB_c}{u_oB_o}\frac{u_o^2}{2H_o}\right)\right\} dG, \quad \text{(B10)}$$

where use has been made of the crossover condition $E/u_cB_c = \gamma/(\gamma - 1)$. The shape of the upper branch of the type (b) (B,ρ)-curve is such that $B_o > B_c$ and it follows that the parameter point will move to the right as G is reduced, provided that the expression in braces on the right-hand side of equation (B10) is positive. After further algebra we find

$$\left(\frac{B_o}{B_c} - 1\right) d\left(\frac{G^2H^o}{F^{o2}}\right) =$$

$$-2\frac{GH_op_o}{F^{o3}}\left\{1 + \frac{B_o^2}{2\mu p_o}\left(1 - \frac{\gamma}{2 + (\gamma - 1)M_o^2}\frac{p_c}{p_o}\frac{B_c}{B_o}\right)\right\} dG, \quad \text{(B11)}$$

and it is clear that the expression in braces is positive for P_2, where $p_c = p_o$, $B_c = B_o$ and $M_o = 1$. As equation (B8) shows $G/\sqrt{(\mu F^{o3}/2)}$ decreases with decreasing G, so that moving the

parameter point infinitesimally to the right from P_2 along the sonic-state envelope implies an infinitesimal increase in E^*.

The progression along O_2P_2 and then along the envelope to Q is equivalent to moving up a line of constant β^* in the (β^*,λ^*)-plane of figure 5 from a point on AA' to one on B'A' to one on B'B'', where a sonic exit state (Q) is reached. Thereafter the operating point moves up from Q at constant G^2H^o/F^{o2}, flow being fully subsonic to sonic exit. The progression ends when the KKS limit is reached. The case of P_2 coinciding with Q is equivalent to having a β^* = const. line passing through B', and the result that β^* = 7 there (see figure 5) is easily recovered from the slope $\sqrt{(2\mu F^o/B^2)}$ being $\sqrt{(3/2)}$ - see property (iii) above. The point B'' corresponds to the KKS limit being at Q

---

* We have found no simple method of demonstrating that the expression in braces is positive for finite displacement of the parameter point. B_c/B_o is less than unity, as is $\gamma/[2 + (\gamma - 1)M_o^2]$. It is easily shown that at the KKS limit p_c/p_o varies from $32(\gamma - 1)/15$, which would be greater than unity for $\gamma <$ 17/15, at B'' to a value less than unity at A'', but the product of the three quantities is less than unity throughout that range for any reasonable value of γ. It may also be shown that loci of constant pressure in the (H,F)-plane are parabolas with axes parallel to the hypersonic-state line (p = 0), but displaced downwards and to the left. They touch the sonic-state parabola and it follows that a process parabola with $p = p_c$ at a crossover point lies very close to the $p = p_c$ line to the left of the crossover. The pressure variation is therefore small.

and using equation (B9) and properties given under (ii) above, the result that $B_o^2/2\mu p_p = 27/5$ there (see the paragraph following equation (33) of §4) is also recovered.

Further increase in the value of the magnetic field at duct inlet leads to the parameter point for a magnetosonic state moving along the magnetosonic line to the intersection of that line with the sonic-state envelope. The parameter point then corresponds to A' in the (β^*,λ^*)-plane of figure 5 with the sonic inlet being also a crossover. There is, however, the possibility of maintaining the operating point at that intersection while reducing the inlet Mach number, giving conditions corresponding to the line A'A'' on figure 5. For $\gamma = 4/3$, the intersection point has parameter values $G^2H^o/F^{o2} = 0.7042$ and $GE/\sqrt{(\mu F^{o3}/2)} = 0.7368$, from which the results given on figure 5, $\beta^* = 16.19$ at A' and 29.36 at A'', may be recovered.

We are now in a position to consider whether the occurrence of hypersonic states causes causes a limitation to possible flow processes in the MHD duct. Consider the $(G^2H^o/F^{o2}, GE/\sqrt{(\mu F^{o3}/2)})$ -plane with both sonic-state and hypersonic-state envelopes. The latter will be reduced in size by comparison with the former by the factor $\gamma^2/(\gamma^2 - 1)$. Evaluating the co-ordinates of the intersection point of the two envelopes gives $G^2H^o/F^{o2} = 0.6050$. This intersection therefore lies to the left of the intersection between the sonic-state envelope and the magnetosonic line (see above). Since all parameter points which give satisfactory operating conditions lie above and to the right of the latter intersection, they must lie outside the hypersonic-state envelope. Inspection of figure B1 shows that there can then

only be a hypersonic-state on the (B,ρ)-curves associated with such parameter points if the curves are of type (a) with an upper branch or of type (c) or of type (b) and that there cannot be more than one. They are the hypersonic states given by the intersection of process parabolas with the hypersonic line at the bottom left-hand corner of the (H,F)-plane (see figure A4) and have no significance for the present MHD duct flows.

REFERENCES

COWLEY, M.D. 1963 *J.Fluid Mech.* **15**, 577.

COWLEY, M.D. 1967 *J.Plasma Physics.* **1**, 37.

SHERCLIFF, J.A. 1958 *J.Fluid Mech.* **3**, 645.

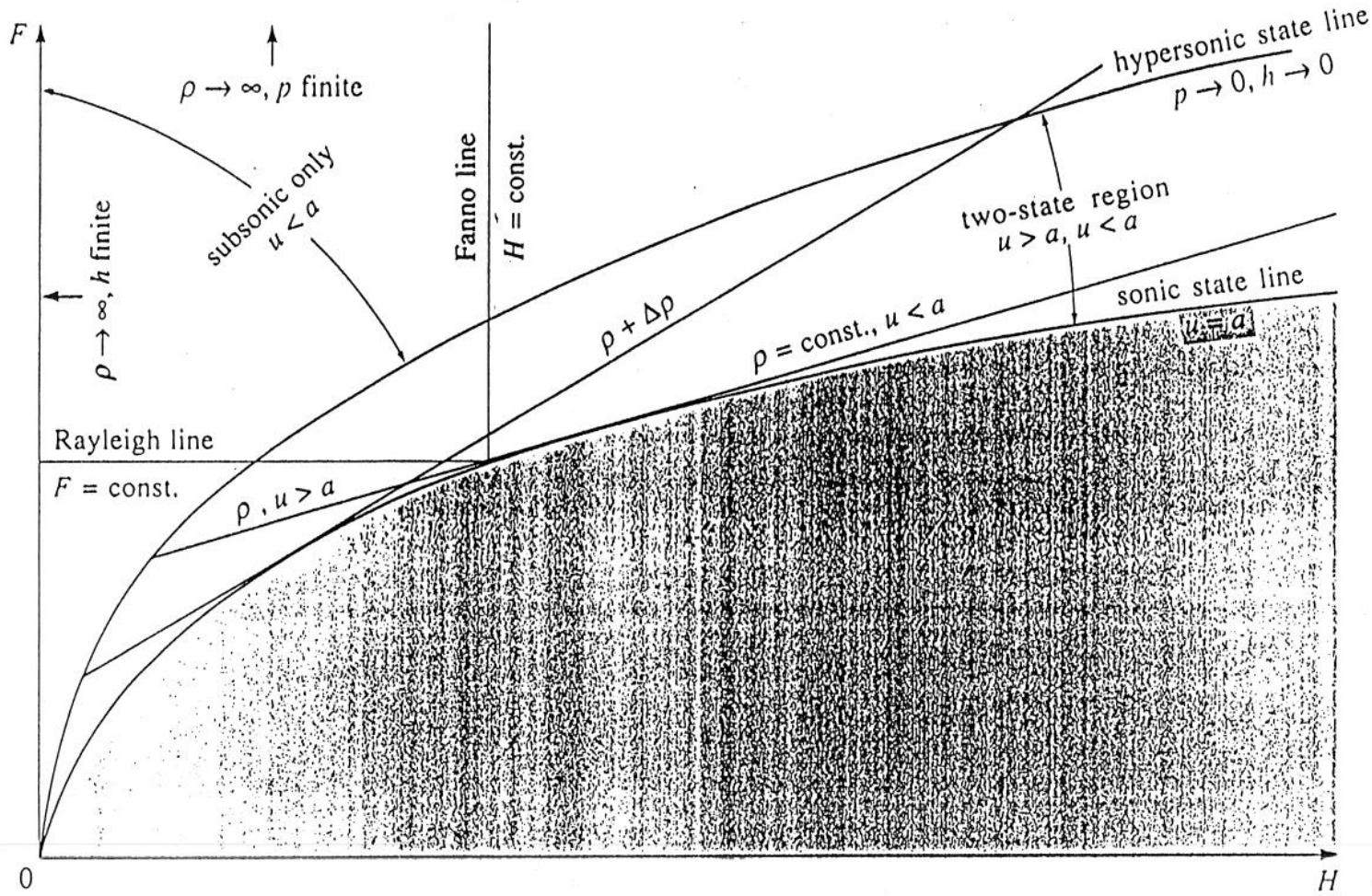

Figure A1. The (H,F)-plane for one-dimensional gasdynamic processes with G = const.

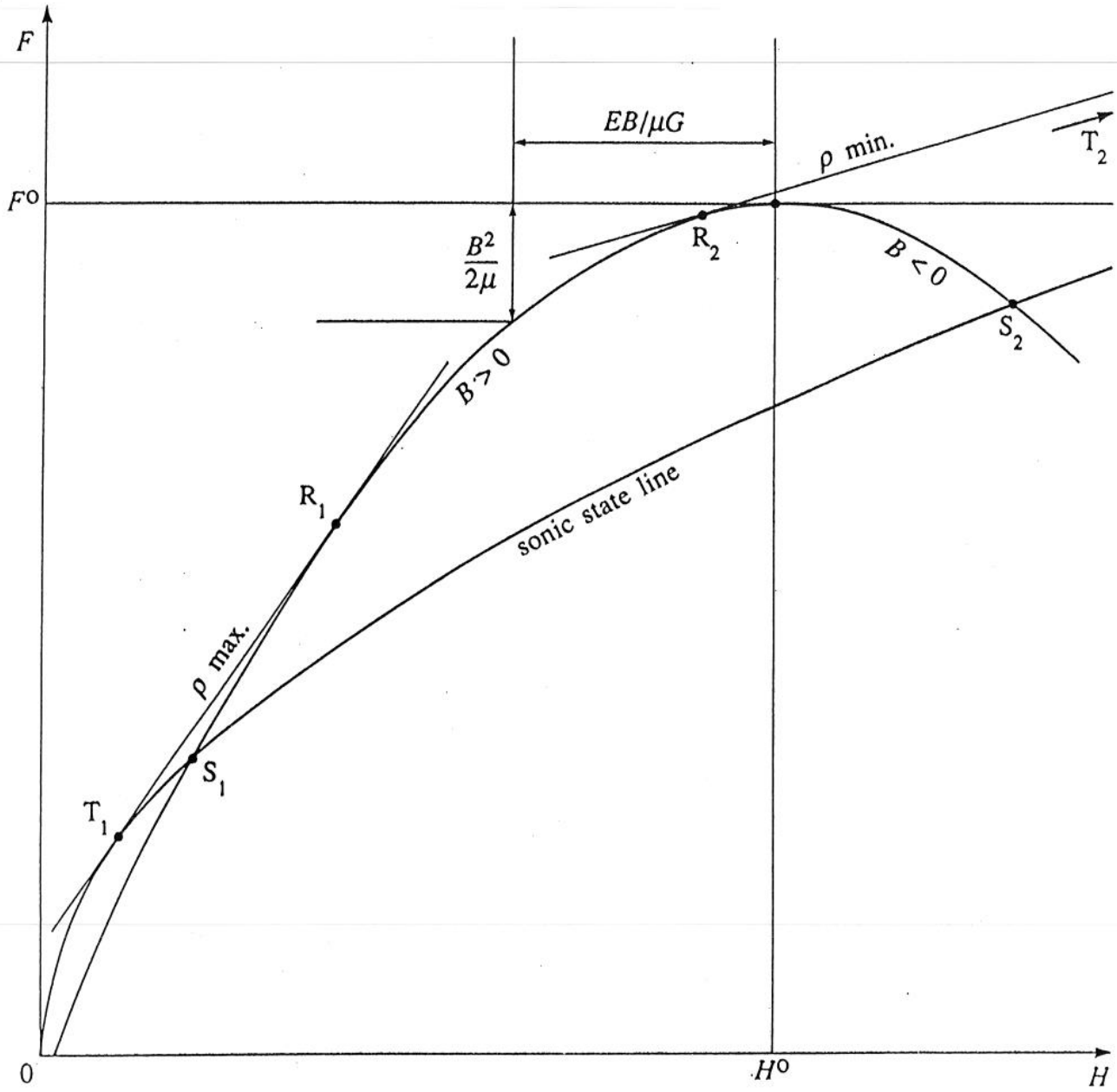

Figure A2. A process parabola on the (H,F)-plane.

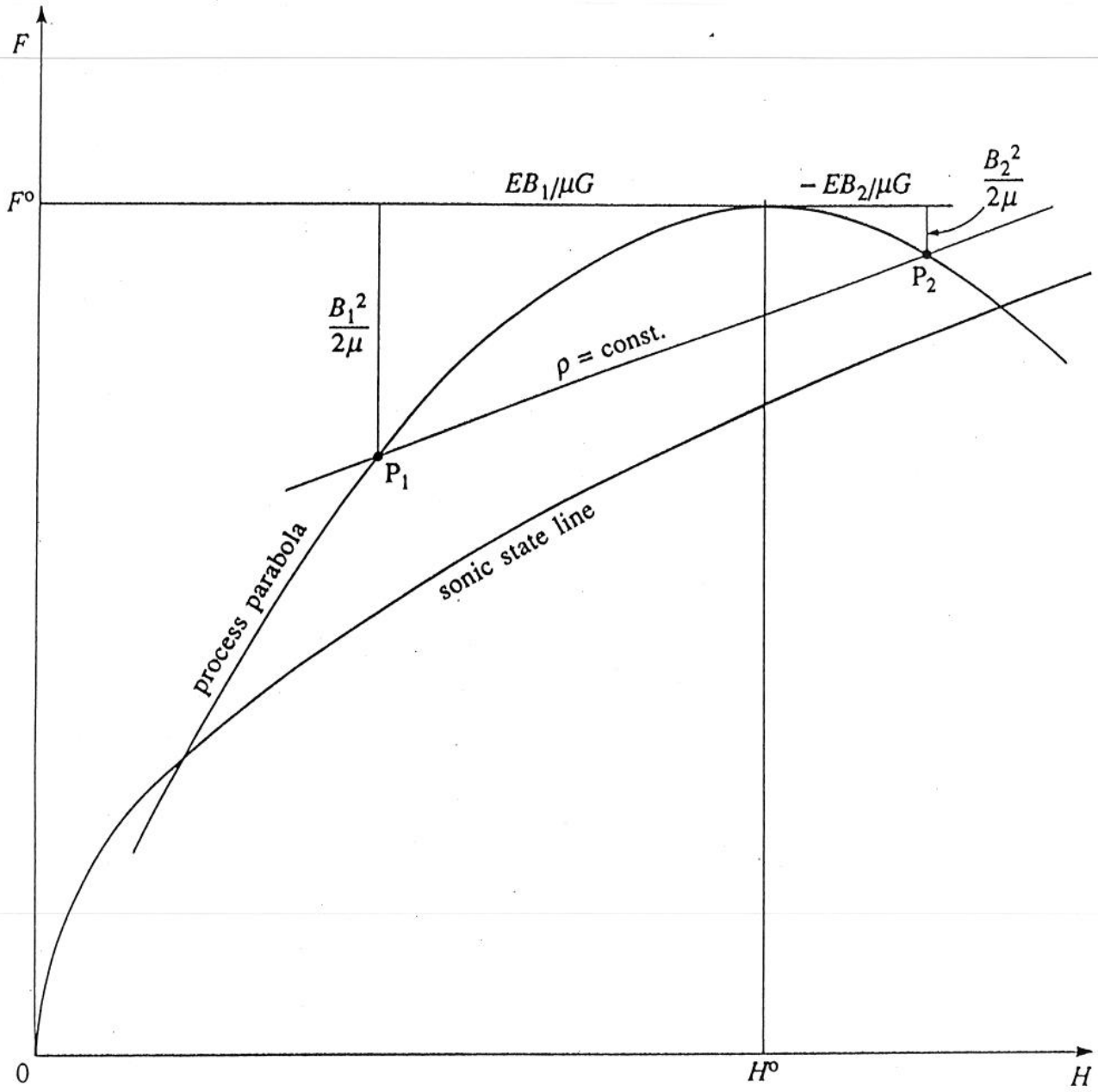

Figure A3. Diagram for relating $(B_2 + B_1)/2$ to $(E\rho/G)(\gamma - 1)/\gamma$.

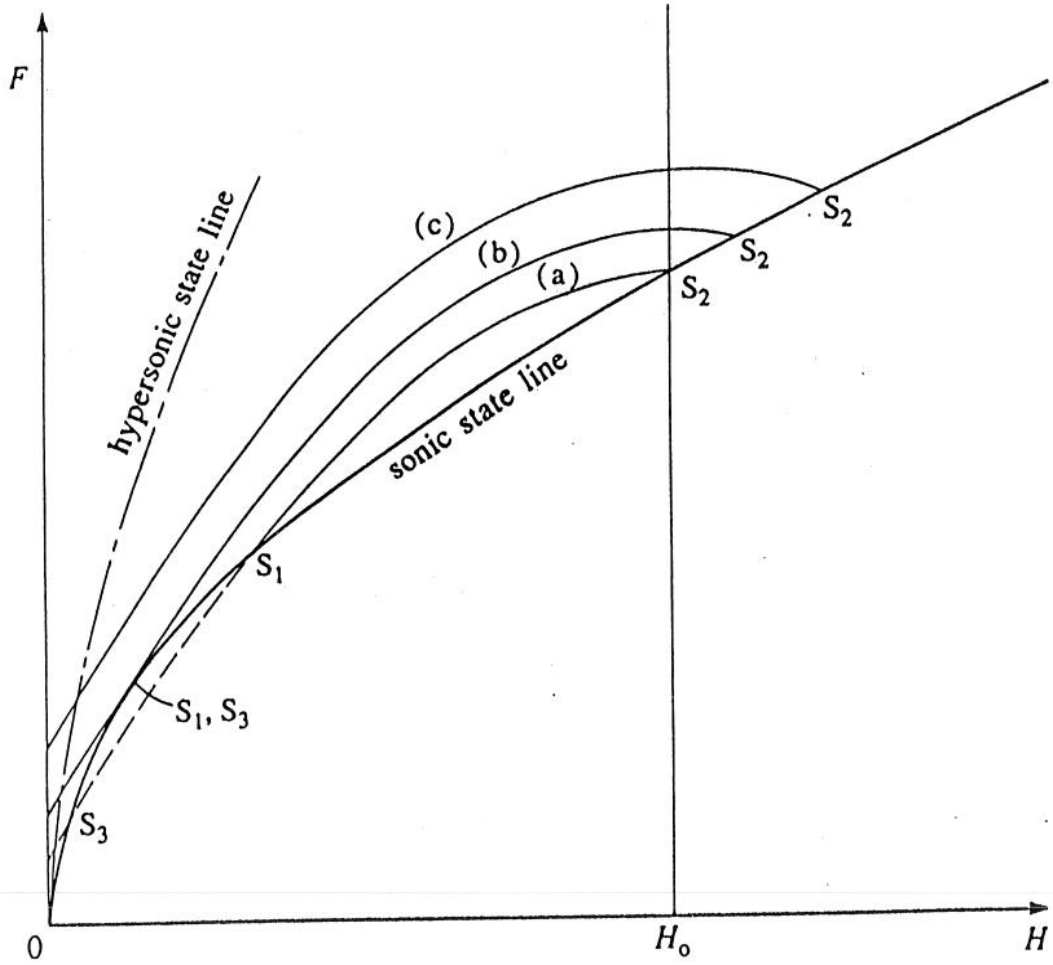

Figure A4. Family of process parabolas for H^o and G/E constant.

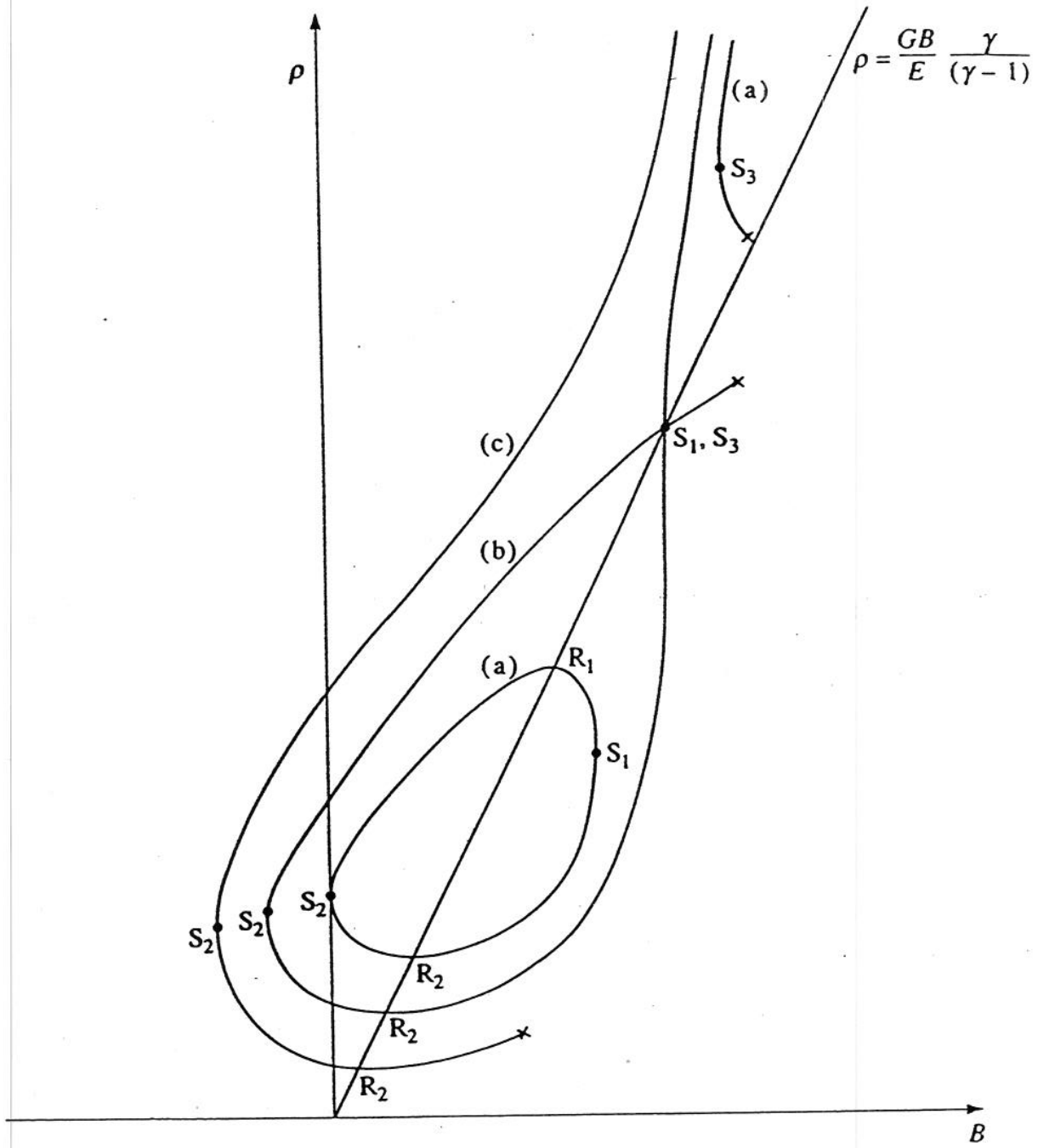

Figure A5. The (B,ρ)-curves corresponding to the family shown on the (H,F)-plane in figure A4. •, sonic point; X, hypersonic point.

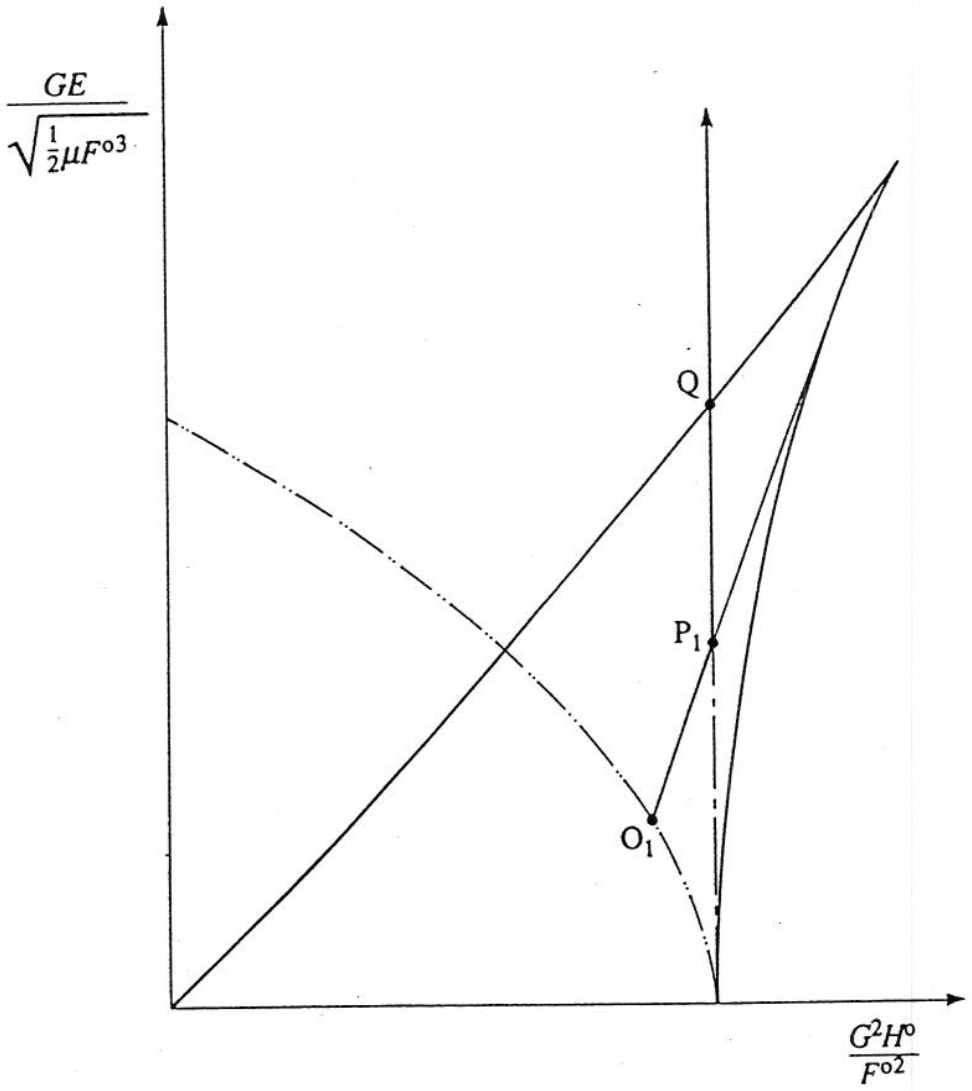

Figure B2. The locus of parameters for particular plenum-chamber conditions and value of magnetic field at duct inlet. On O_1P_1 the inlet condition is sonic with $B_o^2/2\mu F^o$ less than 1/3, exit supersonic. On P_1Q and its continuation the inlet condition is subsonic, exit sonic. - ·· -, magnetosonic line.

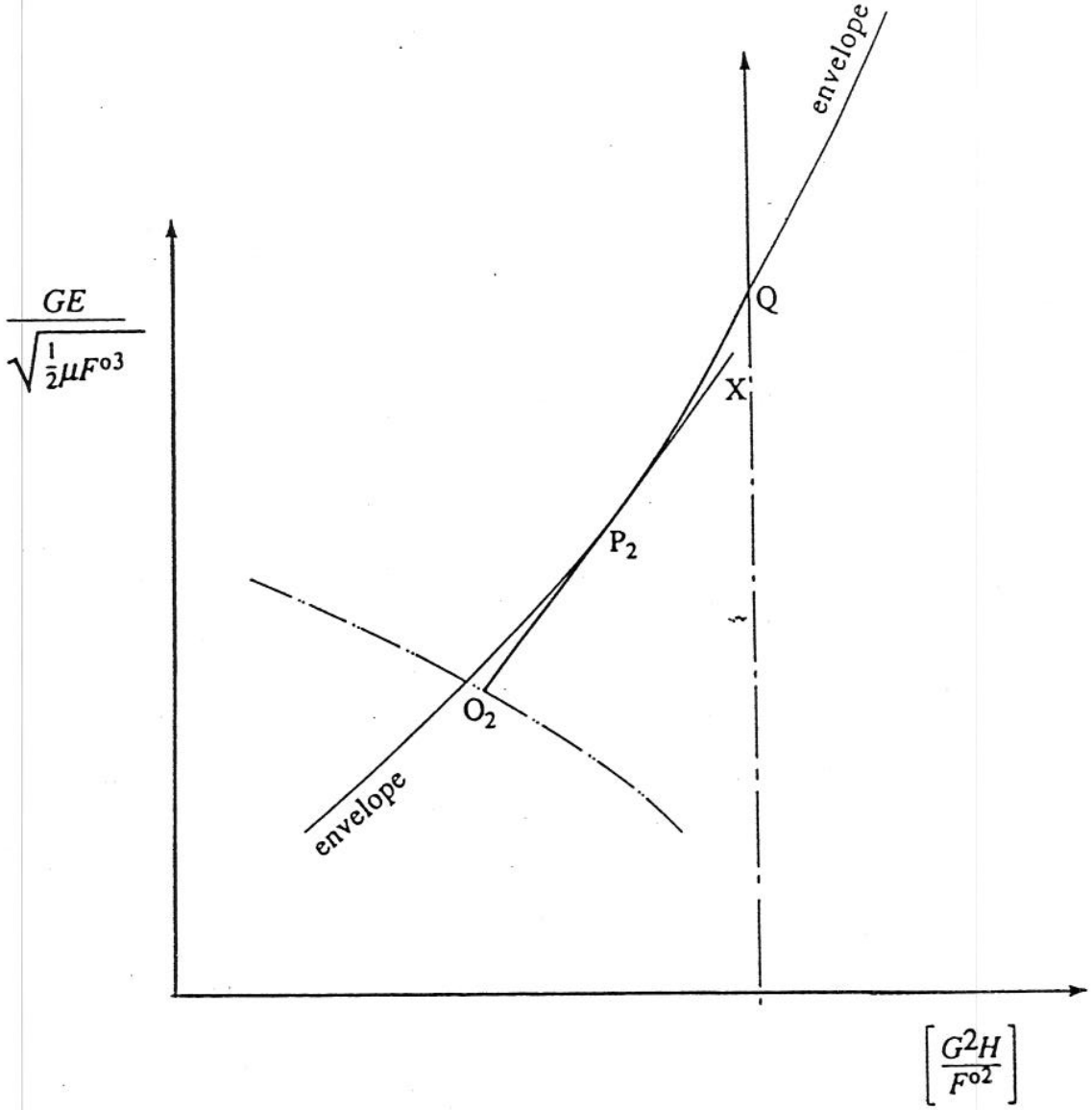

Figure B3. The locus of parameters for particular plenum-chamber conditions and value of magnetic field at duct inlet. Note that O_2P_2X is a straight line, being tangent to the sonic-state envelope at P_2. Between O_2 and P_2 the inlet condition to the duct is sonic.with $B_o^2/2\mu F^o$ greater than 2/3, exit supersonic. On the sonic-state envelope between P_2 and Q the inlet condition is subsonic, exit supersonic. From Q upwards the inlet condition is subsonic, exit sonic. X is a prohibited point for the given plenum-chamber conditions. - ·· -, magnetosonic line.